

# CONTINUOUS FLOW “RAIL-AND-TRAP” MICROFLUIDIC PROCESSORS FOR AUTONOMOUS BEAD-BASED MIXING AND VISUALIZATION

Ryan D. Sochol<sup>\*,†</sup>, William E. R. Krieger<sup>†</sup>, Mengqian Liu, Sarah Hesse,  
Jonathan Lei, Luke P. Lee and Liwei Lin

Berkeley Sensor and Actuator Center, University of California, Berkeley, USA

<sup>†</sup>These authors contributed equally to the manuscript

## ABSTRACT

Multi-stage fluidic mixing reactions are critical to diverse chemical and biological assays (*e.g.*, immunoassays). Unfortunately, the majority of such assays suffer from laborious and time intensive fluidic mixing procedures. Although microfluidic platforms offer significant advantages for accomplishing biochemical assays, current systems primarily require external regulation during device operation, particularly for cases in which microbead visualization is desired or required during intermediate stages of reaction processes (*e.g.*, aptamer-based sandwich assays). To overcome these limitations, here we present a microfluidic “rail-and-trap” processor that functions autonomously under continuous input flow conditions to both: (i) perform multi-step fluidic mixing routines with suspended microbeads, and (ii) immobilize select numbers of microbeads for visualization and/or optical detection during each step of multi-stage fluidic processes. Experimental results revealed railing efficiencies and trapping efficiencies of 100% for the prototype system, with microbead visualization achieved during each fluidic mixing stage.

## KEYWORDS

Railing, Microbeads, Trapping, Continuous Flow

## INTRODUCTION

Microfluidic technologies that employ microbeads as reaction substrates offer significant advantages for accomplishing biochemical assays, including low reagent volumes, high surface-to-volume ratios, enhanced reaction kinetics, and the ability to mix-and-match microbeads corresponding to specific screenings [1-3]. In addition, microbeads can be functionalized with diverse surface modifications, such as molecular probes capable of detecting DNA analytes and inflammatory cytokines [4, 5]. The majority of bead-based microfluidic technologies, however, require external observation and/or regulation during device operation to perform multi-stage fluidic mixing and assaying procedures. Consequently, recent research has focused on developing systems with autonomous “on-chip” functionalities [6-9]. Continuous flow methodologies (*e.g.*, microfluidic railing techniques) offer powerful means for transporting microparticulates into discrete, parallel flow streams to rapidly execute mixing routines [10-13]. For example, researchers have successfully demonstrated microfluidic railing of microdroplets using comparatively smaller microposts (alternatively referred to as micropillars) [12, 13]. Previously, we presented the first microfluidic system capable of railing not only suspended microbeads, but also suspended cells; however, microbead visualization (and therefore, fluorescence detection) was not possible until after completion of the full reaction process [14, 15]. To overcome this drawback, here we adapt our prior technique in order to enable microbead immobilization and visualization during each step of multi-stage fluidic mixing processes (Fig. 1).

## CONCEPT

Conceptual illustrations of the microfluidic rail-and-trap system are shown in Figure 1. Previously, we observed that square microposts arrayed at an angle of  $1^\circ$  successfully railed microbeads; however, higher angles (*e.g.*,  $10^\circ$ ) were found to induce microbead immobilization in the gaps between microposts [14, 15]. In this work, we exploit these phenomena in order to passively: (i) transport suspended microbeads into distinct, parallel flow streams, and (ii) immobilize select numbers of microbeads during each fluidic mixing stage. The microfluidic rail-and-trap

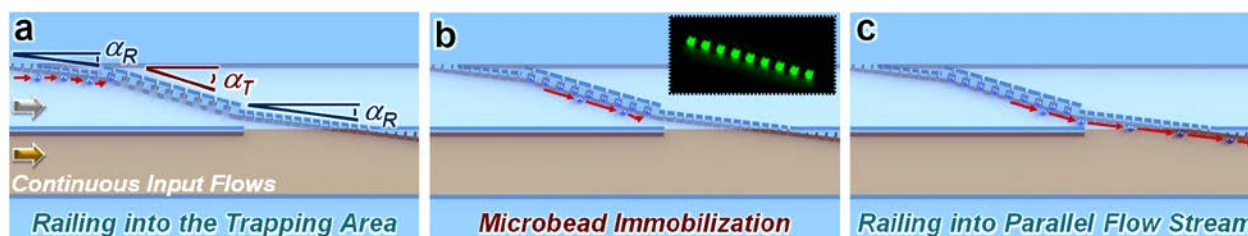


Figure 1. Conceptual illustrations of the microfluidic “rail-and-trap” system. (a) Under continuous input flow conditions, microposts arrayed at a low railing angle,  $\alpha_R$ , guide suspended microbeads into the trapping area. (b) The higher trapping angle,  $\alpha_T$ , promotes microbead immobilization in the designated trapping positions. (Inset) Microbead immobilization enables fluorescence detection during each step of multi-stage mixing reactions. (c) After each trapping site is occupied by a microbead, subsequent beads are transported into the adjacent fluidic stream via the micropost array rails. This process can be repeated as desired (*e.g.*, with additional reagents and/or washes continuously loaded in parallel) to autonomously accomplish diverse bead-based fluidic mixing reactions.

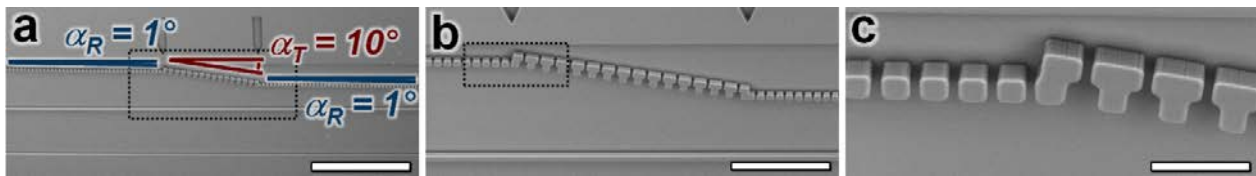


Figure 2. SEM micrographs of fabrication results for the microfluidic “rail-and-trap” system with  $\alpha_T = 10^\circ$  and  $\alpha_R = 1^\circ$ . Scale Bars = (a) 500  $\mu\text{m}$ , (b) 200  $\mu\text{m}$ , and (c) 50  $\mu\text{m}$ .

system consists of square-shaped microposts (*i.e.*, of approximately the same size as the microbeads) that are arrayed in sections at a low angle,  $\alpha_R$ , and ‘T’-shaped traps that are arrayed at a higher angle,  $\alpha_T$ , in order to prevent or promote microbead immobilization, respectively. Under continuous input flow conditions, microbeads are initially guided toward the trapping area due to the low  $\alpha_R$  (Fig. 1a). The higher  $\alpha_T$  promotes microbead immobilization in the designated ‘T’-shaped trapping positions (Fig. 1b), which enables fluorescence detection (Fig. 1b – *inset*). The ‘T’-shaped trapping designs were used to preclude microbead immobilization prior to the trapping area [16]. After immobilizing one microbead in each trapping site, subsequent beads are transported into the adjacent fluidic stream (Fig. 1c). This process can be repeated continuously as desired. For example, additional fluidic reagents and washes can be inputted in parallel to tailor the rail-and-trap system for diverse fluidic mixing processes, while enabling microbead visualization and optical detection during each step of such multi-stage reactions.

### MICROFABRICATION

The prototype rail-and-trap system was fabricated *via* standard single-layer soft lithography processes using polydimethylsiloxane (PDMS) as described previously [14-16]. The devices included arrays of square-shaped microposts ( $15 \times 15 \mu\text{m}^2$ ), with an interpost spacing of 5  $\mu\text{m}$ . The microchannels were 18  $\mu\text{m}$  in height. A total of three testing systems were constructed, corresponding to three different values of  $\alpha_T$  (*i.e.*,  $10^\circ$ ,  $15^\circ$ , and  $20^\circ$ ). Figure 2 shows microfabrication results for a system with  $\alpha_T = 10^\circ$  and  $\alpha_R = 1^\circ$ .

### RESULTS

Experiments with suspended streptavidin-coated polystyrene microbeads (15  $\mu\text{m}$  in diameter) were performed using testing systems with varying  $\alpha_T$  (*i.e.*, while  $\alpha_R$  was held constant at  $1^\circ$ ) in order to investigate the effects of  $\alpha_T$  on both the railing and trapping performance. In this study, a clear microbead suspension and an orange-dyed solution of phosphate buffered saline (PBS) were continuously loaded in parallel *via* syringe pumps set at 1.5  $\mu\text{l}/\text{min}$ . For testing systems in which  $\alpha_T$  was too high (*i.e.*,  $\alpha_T \geq 15^\circ$ ), microbeads were not only observed to immobilize in the designated trapping positions, but also on top of previously arrayed beads as well as in the  $\alpha_R$  railing area directly preceding the traps. These issues resulted in device failure because subsequent microbeads were prevented from bypassing fully occupied trapping areas, leading to the loss of high numbers of microbeads within such systems. In contrast, experiments revealed that the prototype system with  $\alpha_T = 10^\circ$  (and  $\alpha_R = 1^\circ$ ) effectively immobilized select numbers of microbeads in the designated array positions, while transporting all of the subsequent microbeads into the distinct, parallel flow streams as designed. For example, Figure 3a-d show suspended microbeads being: (a) railed into the  $\alpha_T$  trapping area for immobilization, (b) transported along the micropost array rails from the clear solution into the discrete, adjacent orange solution, (c) directed to bypass previously immobilized microbeads in the  $\alpha_T$  trapping area, and (d) transported along the micropost array rails from the orange solution back to the parallel clear solution. Multiple experimental device runs confirmed that this process was repeatable. Quantified results for this microfluidic rail-and-trap system revealed a railing efficiency of 100% (*i.e.*, microbeads were not found to immobilize in the  $\alpha_R$  railing sections) and a ‘one-bead-per-trap’ trapping efficiency of 100%. Additionally, as shown in Figure 3e and f, the microfluidic rail-and-trap system enabled both brightfield observation (*top*) and fluorescence visualization (*bottom*) of arrayed microbeads during each fluidic mixing stage.

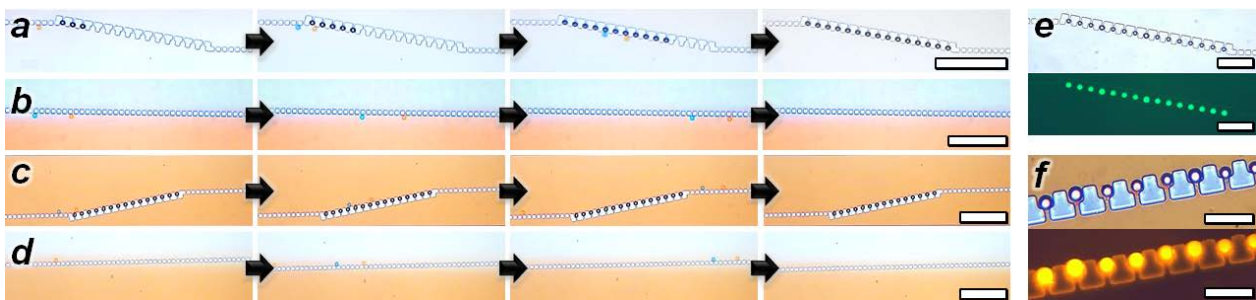


Figure 3. Experimental results for the continuous flow microfluidic rail-and-trap system with  $\alpha_T = 10^\circ$  and  $\alpha_R = 1^\circ$ . (a) Microbeads are railed into the trapping area and then immobilized. (b) A microbead is railed from the clear solution into the orange solution. (c) A microbead is railed past previously immobilized beads. (d) A microbead is railed from the orange solution back to the clear solution. (e, f) Brightfield and fluorescence micrographs of immobilized microbeads. Microbeads are 15  $\mu\text{m}$  in diameter; ‘Blue’ and ‘orange’ colored microbeads show a single bead captured at two time points within one second. Scale Bars = (a-d) 200  $\mu\text{m}$ , (e) 100  $\mu\text{m}$ , (f) 50  $\mu\text{m}$ .

## CONCLUSIONS

Microfluidic technologies that are capable of autonomous on-chip functionalities are critical to the advancement of lab-on-a-chip applications, such as point-of-care (POC) molecular diagnostics and biomarker screening. In this work, we presented a continuous flow microfluidic system that utilized microposts and ‘T’-shaped traps arrayed at angles of  $1^\circ$  and  $10^\circ$  (*i.e.*, with respect to the flow direction), respectively, in order to passively perform multi-step fluidic mixing operations, while immobilizing select numbers of microbeads during each mixing stage. Experimental testing revealed that trapping areas with higher angles (*i.e.*,  $\alpha_T \geq 15^\circ$ ) resulted in device failure because subsequent microbeads were unable to effectively bypass previously arrayed beads. Such systems were found to cause microbeads to immobilize on top of previously trapped microbeads as well as in the  $\alpha_R$  railing section prior to the trapping areas. In contrast, systems that included trapping areas with ‘T’-shaped traps arrayed at an angle of  $10^\circ$  were found to effectively rail-and-trap the microbeads as designed. Experimental device runs revealed railing and trapping efficiencies of 100%, with brightfield and fluorescence visualization of arrayed microbeads accomplished during each fluidic mixing step. These results suggest that the presented continuous flow microfluidic rail-and-trap system offers a robust single-layer platform for passively executing multi-stage fluidic mixing procedures with suspended microbeads (*e.g.*, for chemical and biological assays), with the unique capability of enabling microbead visualization and signal detection during each stage of multi-step reaction processes.

## ACKNOWLEDGEMENTS

The authors greatly appreciate the help and support of Thomas Brubaker, Kosuke Iwai, Albert Lu, Casey Glick, Nazly Pirmoradi, Adrienne Higa, and Paul Lum, as well as the members of the Liwei Lin Laboratory, the Biologically-inspired Photonics-Optofluidics-Electronics Technology and Science (BioPOETS) Laboratory, and the Micro Mechanical Methods for Biology (M<sup>3</sup>B) Laboratory. This research is supported in part by the DARPA N/MEMS program under the Micro/Nano Fluidics Fundamentals Focus (MF3) center.

## REFERENCES

- [1] W. H. Tan and S. Takeuchi, *A trap-and-release integrated microfluidic system for dynamic microarray applications*, Proc. of the National Academy of Sciences of the United States of America, pp. 1146-1151, (2007).
- [2] E. Verpoorte, *Beads and chips: new recipes for analysis*, Lab on a Chip, pp. 60N-68N, (2003).
- [3] K. Iwai, W. H. Tan, H. Ishihara, and S. Takeuchi, *A resettable dynamic microarray device*, Biomedical Microdevices, pp. 1089-1094, (2011).
- [4] R. D. Sochol, B. P. Casavant, M. E. Dueck, L. P. Lee, and L. Lin, *A dynamic bead-based microarray for parallel DNA detection*, Journal of Micromechanics and Microengineering, p. 054019, (2011).
- [5] N. Tuleuova, C. N. Jones, J. Yan, E. Ramanculov, Y. Yokobayashi, and A. Revzin, *Development of an Aptamer Beacon for Detection of Interferon Gamma*, Analytical Chemistry, 82, pp. 1851-1857, (2010).
- [6] D. C. Leslie, C. J. Easley, E. Seker, J. M. Karlinsey, M. Utz, M. R. Begley, and J. P. Landers, *Frequency-specific flow control in microfluidic circuits with passive elastomeric features*, Nature Physics, pp. 231-235, (2009).
- [7] J. A. Weaver, J. Melin, D. Stark, S. R. Quake, and M. A. Horowitz, *Static control logic for microfluidic devices using pressure-gain valves*, Nature Physics, pp. 218-223, (2010).
- [8] B. Mosadegh, C.-H. Kuo, Y.-C. Tung, Y.-S. Torisawa, T. Bersano-Begey, H. Tavana, and S. Takayama, *Integrated elastomeric components for autonomous regulation of sequential and oscillatory flow switching in microfluidic devices*, Nature Physics, pp. 433-437, (2010).
- [9] B. Mosadegh, T. Bersano-Begey, J. Y. Park, M. A. Burns, and S. Takayama, *Next-generation integrated microfluidic circuits*, Lab on a Chip, pp. 2813-2818, (2011).
- [10] S. A. Peyman, A. Iles, and N. Pamme, *Rapid on-chip multi-step (bio)chemical procedures in continuous flow – manoeuvring particles through co-laminar reagent streams*, Chemical Communications, pp. 1220-1222, (2008).
- [11] S. E. Chung, W. Park, S. Shin, S. A. Lee, and S. Kwon, *Guided and fluidic self-assembly of microstructures using railed microfluidic channels*, Nature Materials, pp. 581-587, (2008).
- [12] C. Kantak, S. Beyer, L. Yobas, T. Bansal, and D. Trau, *A ‘microfluidic pinball’ for on chip generation of layer-by-layer polyelectrolyte microcapsules*, Lab on a Chip, pp. 1030-1035, (2011).
- [13] S. Zhang, L. Yobas, and D. Trau, *A microfluidic device for continuous flow layer-by-layer encapsulation of droplets with polyelectrolytes*, Proc. of the 12th International Conference on Miniaturized Systems for Chemistry and Life Sciences (MicroTAS 2008), pp. 1402-1404, (2008).
- [14] R. D. Sochol, R. Ruelos, V. Chang, M. E. Dueck, L. P. Lee, and L. Lin, *Continuous flow layer-by-layer microbead functionalization via a micropost array railing system*, Proc. of the 16th International Solid-State Sensors, Actuators and Microsystems Conference (Transducers 2011), pp. 1761-1764, (2011).
- [15] R. D. Sochol, S. Li, L. P. Lee, and L. Lin, *Continuous Flow Multi-Stage Microfluidic Reactors via Hydrodynamic Microparticle Railing*, Lab on a Chip, (2012). (DOI: 10.1039/C2LC40610A)
- [16] R. D. Sochol, W. E. R. Krieger, L. P. Lee, and L. Lin, *Autonomous railing and trapping of microbeads for continuous flow multi-stage microfluidic processes*, Proc. of the IEEE Solid-State Sensor and Actuator Workshop (Hilton Head 2012), (2012).

## CONTACT

\*Ryan D. Sochol, tel: +1-410-935-8971; rsochol@gmail.com